LOW-COST, SINGLE PLATFORM, HYBRID MANUFACTURING OF RF PASSIVES

A Thesis
Presented to
The Academic Faculty

by

Daniel L. Revier

In Partial Fulfillment
of the Requirements for the Degree
Master of Science in the
School of Electrical and Computer Engineering

Georgia Institute of Technology
August 2016

LOW-COST, SINGLE PLATFORM, HYBRID MANUFACTURING OF RF PASSIVES

Approved by:

Professor Emmanouil Tentzeris, Advisor
School of Electrical and Computer Engineering
Georgia Institute of Technology

Professor Andrew Peterson
School of Electrical and Computer Engineering
Georgia Institute of Technology

Professor Gregory Durgin
School of Electrical and Computer Engineering
Georgia Institute of Technology

Date Approved: July 27, 2016

To my mother and father, Sharon and David,

to my soon-to-be wife, Eden Morris,

& to all my friends along the way that helped me get here.

ACKNOWLEDGEMENTS

First, I would like to thank my fiancee Eden Morris, without whom I'd likely not have ended up in Georgia at all. She has been with me every step of the way through this ridiculous journey of simultaneously working and attending school. It hasn't always been easy, but it has certainly always been well worth it.

I want to thank my advisor, Dr. Tentzeris. Without his understanding and encouragement throughout the work/school process I would have likely found it much easier to quit and pack up my bags than press on with this work. The ATHENA lab was always a huge support and full of great ideas and a passion for printing the world. A special thanks to Benjamin Cook for seeing potential in me and helping me find my way in the world of additive manufacturing. I'd also like to thank Drs. Peterson and Durgin for being excellent professors and helping me both in the classroom and the lab.

Hyrel 3D also deserves special thanks. The Hyrel team was always responsive, courteous and more than willing to make time for me from the first moment I contacted them to every support call I had with them. They entertained my ideas for printed antennas and truly wanted to see me succeed. The support I received from them goes far beyond technical nature of this work. A tremendous amount of this success was helped by the hands of Karl, Davo and the rest of their team.

Finally, I'd like to thank everyone at GTRI for helping fostering my curiosity for RF design and allowing me to talk far too much about printed RF antennas. My work at GTRI directly contributed to this research and as such I would be remiss to forget the massive impact they had. To James Skala, Roger Hasse, Glenn Hopkins, Alyssa Daya, Ben Riley and Kathy Harger, thank you all so, so very much.

TABLE OF CONTENTS

LIST OF TABLES

LIST OF FIGURES

SUMMARY

The research provided in this thesis focuses on the development of a low-cost, single-platform hybrid manufacturing process for realizing canonical and wideband antenna structures. This work outlines the printing processes of thick dielectrics & thin metallic geometries in coordination with selective removal of planar copper structures and provides a proof-of-concept demonstration of the first hybrid manufactured RF structures. Using the outlined processes, demonstrations of a 6 GHz inset patch feed antenna and a wideband Vivaldi array are presented as a first of their kind approach to realizing RF passive radiators.

Chapter 1 introduces the concept and general benefits of hybrid manufacturing over isolated use of additive or subtractive manufacturing and outlines the steps required to realize hybrid manufactured RF electronics.

Chapter 2 gives a brief description of various attempts to fabricate additive manufactured RF electronics, their benefits and detractions.

Chapter 3 introduces the platform, materials, and specific process details to be used.

Chapter 4 presents the design, fabrication and measurement of the printed patch antenna and Vivaldi antenna array.

Finally, Chapter 5 summarizes the contributions of the work within this thesis.

CHAPTER I

INTRODUCTION

It would not be an outrageous statement to claim that additive manufacturing (AM) stands at a point ready to impact nearly every object encountered today. This is in part due to the breadth of the manufacturing process that additive technology touches (e.g. prototyping, rapid tooling) but also due to the inherent cost-saving nature of selectively depositing materials. That being said, AM is, in itself, not the be-all-end-all that many blogs, magazines and even academic publications make it out to be. While it does offer many benefits, it will not replace traditional (a.k.a. subtractive) manufacturing technologies wholesale. In fact, this research demonstrates that through a blending of both additive and subtractive technologies, a hybrid manufacturing (HM) approach to low-cost, single-platform device construction is the ideal method of realizing and prototyping RF passives.

This research proposes to address the issues specifically tied to material extrusion (ME) manufacturing, which is a branch of AM that focuses on single-point deposition of material by extruding a material through a nozzle. The major issues with ME, as highlighted by [12, Chapter 6], are as follows:

1. Build speed, which is dependent on the feed rate and the print speed
2. Accuracy, which is dependent on the nozzle size and motor drive systems
3. Material density, which is dependent on proper tool path planning and tool calibration

All told, these issues lead to inefficient printing of large structures, poor resolution due to nozzle deposition size, and a higher cost of complicated materials needed for

the ME deposition process. Some attempts have been made to address these issues individually (e.g. multiple parallel nozzles, smaller nozzle diameter), but up until this point there has not been an attempt to address these pitfalls on a single-platform.

1.1 Research Objectives

The objective of this proposed research is to put forth an inherently low-cost hybrid manufacturing process that can be adjusted to improve quality, decrease per unit cost and lower fabrication time of printed RF passives. In essence, the process is boiled down into three individual steps:

1. Polymer deposition
2. Silver deposition
3. Copper subtraction

Each of these three steps can be combined in any order to produce complicated multi-layer RF structures. Examples will be provided later to illustrate the necessary order and combination of the steps to produce some standard RF radiators.

Altogether, AM is a novel technology that stands to become indispensable in the future of general manufacturing. Until this point, AM has been generally operated in isolation of other manufacturing technologies. This research proposes the novel combination of both additive and subtractive manufacturing technologies to produce a hybrid manufacturing process through silver and polymer deposition, with copper tape subtraction. This in turn will help reduce the cost of printed electronics structures, increase resolution and reduce the time for production of the items.

1.2 Thesis Outline

This thesis is outlined as follows:

1. Chapter 2 briefly describes recent investigations into 3D printed RF components and the variety of printing techniques used.

2. Chapter 3 introduces the platform, materials, and specific printing/subtractive processes that are used in this work.

3. Chapter 4 presents the design, fabrication and measurement of a printed patch antenna and a Vivaldi antenna array prototype.

4. Chapter 5 concludes the results of this research.

CHAPTER II

PRIOR ART

Explorations into the RF domain have increased as additive manufacturing technology has improved. A wide variety of different additive technologies are being explored (e.g. inkjet, material extrusion, stereolithography) with each offering distinct benefits. RF applications range from printed circuits to metamaterials. For this thesis, the investigation of prior work focuses on methods that combine printed metals and dielectrics.

Until recently, that research has been dominated by inkjet technology due to its wide material support and fast nature. Inkjet printing technology has matured over the past 30-40 years, is well understood, and supported by a wide variety of materials companies that are able to produce traditional and specialty metal/dielectric inks (e.g. Micochem Sun Chemical & 20+ others) [14]. Inkjet printed antennas/metamaterials/circuits spanning L-band to mm-Wave frequencies have been demonstrated and have shown promise as low-cost package embedded radiators and passives [5, 20, 4, 3, 6]. These are inherently low-profile antennas as the mass throughput via inkjet printed technology is very low. This makes printing structures of an appreciable thickness (>50 μm) very difficult. An ideal case would combine both dielectric and metal printing on a single platform. At the time of this writing, there is an Israeli company that is currently developing an inkjet based electronics printer on a single platform [13]. This approach stands to be highly competitive if the material properties (e.g. conductivity of metal, real/imaginary permittivity of dielectrics) can be brought into the realm of standard RF PCBs.

Higher mass throughput printing techniques, such as material extrusion, must be

used to fabricate larger structures at this time. This is known as fused filament fabrication (FFF) when applied to polymers and "direct write" electronics when applied to printing metals and polymers together. The term direct write comes from the process as the tool passes directly over where the material should be selectively deposited, "writing" in the same manner as a pen or pencil. RF passives fabricated using these techniques have been studied less typically due to machine and material limitations. The printer must be able to simultaneously handle multiple materials that can come in a wide variety of forms (e.g. liquids, solid filaments, suspended colloidal solutions) or multiple printers must be used. Previous investigations into high mass throughput AM electronics are discussed below.

In an early single-platform case, a low-cost (<$5k) ME 3D printer (Ultimaker 2) was retrofitted to accept both dielectric and non-standard conductive material to create RF structures [1, 2] . Both materials were driven through a single nozzle and deposited in successive layers. As a proof of concept, results using this technique exhibited success in both bandwidth and loss; however, components suffered from limited materials selection and poor printing accuracy. Ahmadloo et al. [1, 2] state that a significant amount of time was spent in personally combining a variety of commercial silver inks to be properly extruded. This material blend could be commercially sold; however, it is inherently tied to the Ultimaker extruder and is not transferrable across platforms. Additionally, the silver paste was extruded through the same 0.4 mm printing nozzle as the polymer. This may seem to reduce the complexity of the system and be a superior case single-platform printing, but in reality this introduces nontrivial material mixing between materials. Either the material must be purged before the second material is printed or there will be an amount of time where metal and plastic are combined in printing. Finally, the printed width of the silver must be identical to the polymer width by having a single extrusion point for metals and dielectrics. This will either limit the printed metal resolution (in the case of a large

nozzle) or reduce the mass throughput of the polymer (in the case of a small nozzle) ultimately limiting the applications that this system can satisfy.

On the other end of the cost spectrum, (>$100k) printers (nScrypt nDimension) [17] have been used with great success [8, 11, 9, 18, 16]. Beyond just RF electronics, the nScrypt machine has shown to be an incredibly precise single-platform electronics prototyping machine. [8] proves out several unique examples of fully printed electronics for LED circuits and other general electronics. This is shown as a key example of how additive manufacturing can bring new ideas to embedded electronics. The nScrypt machine is capable of repeatable mechanical performance down to microns and can print a huge variety of materials ranging in viscosity from water to peanut butter. The nScrypt has even been equipped to handle subtractive tools from milling/drilling tools to lasers allowing it to tackle hybrid manufacturing. While the accuracy is impressive and material selection is extremely wide it comes at an obvious high capital expenditure cost making it infeasible and inaccessible for most interested parties.

Conversely, rather than use a single platform it is possible to use multiple printers in a sequential process. This process can be done by manually moving and aligning the component on each tool or it can be done robotically. An investigation was performed combining inkjet printed antennas with ME polymer deposition to combat the inkjet material throughput issues [15]. In this case, the FFF printed substrate was manually moved back and forth between the FFF machine and the inkjet printer. Naturally, this kind of cross-platform printing will introduce registration and alignment errors making it difficult to scale up to higher frequencies. A sophisticated approach to cross-platform printing has been attempted at the University of Texas at El Paso Keck Center for 3D Innovation with repeatable motion in the 10's of microns [7]. This method, while not applied to electronics printing, could easily be envisioned for such a situation. While the cross-platform research has shown promising results, the

ultimate cost comes in the poor process efficiency. At worst, research level manual carrying and aligning of the print will induce human errors that are non-repeatable and inefficient. At best, a robotic arm, like those exhibited at the University of Texas at El Paso, is accurate but ultimately a convoluted approach to serializing different printing techniques.

Finally, the only approach that has come close to achieving the accuracy required for electronics while maintaining an appropriate cost for low-level research is the Voxel8 printer (<$12k) [21]. Voxel8 has produced an electronics prototyping printer that promises low conductor loss and good dielectric properties. Additionally, the accuracy reported for the printer should be able to meet most demanding RF specifications. The Voxel8 shows extreme promise for printed electronics from DC to microwave and potentially beyond; however, at this time it is restricted to just two materials, extruded plastic and printed silver. This makes it a worthwhile investment for electronics but, as will be demonstrated later, does not allow for the novel concept of utilizing different tools for hybrid manufacturing.

In short, there has not been a cost-effective single platform approach to printing electronics that can also produce worthwhile high-quality research RF antennas and passives. A variety of techniques have been studied from retrofitting machines, high-cost machines, and utilizing multiple machines; however, none of these techniques allow for the accuracy and cost that would benefit most applications in the research space. This thesis will demonstrate a process for low-cost, single platform, hybrid manufacturing of RF passives and antennas to fill this gap.

CHAPTER III

HYBRID MANUFACTURING METHODS

The novel manufacturing methods proposed in this thesis have mainly focused on two different areas: Equipment/Materials & Manufacturing Process.

3.1 Equipment & Materials

3.1.1 Hyrel System 30

The Hyrel System 30M, seen in Fig. 1, is a research focused manufacturing platform. No other comparable 3D printer or bench top manufacturing system exists. It has 4 slots that can be equipped with a wide variety of tools. What's more these tools can be easily removed, replaced or swapped around to completely change the function of the printer. Hyrel offers a wide variety of tools for very different tasks; however, only three tools in particular were used for this research as discussed in § 3.1.1.1 and shown in Fig. 2.

3.1.1.1 Tools

The MK1-250 is capable of printing 1.75mm extruded thermoplastic filament for low melting temperature polymers (<250^{o}C). It has a nozzle diameter of approximately 0.5 mm and can print a bead of polymer ranging from 0.3 - 0.7 mm in width and 0.05 - 0.5 mm in height. The minimum vertical layer height is driven predominantly by the non-planarity of the printing bed.

The SDS-5 is a screw driven plunger system designed to be used with standard 5 mL disposable syringes. Any needle size can be used as long as it fits the syringe used. For this research a stainless steel tapered needle (PVA Inc.) with 30 gauge opening (0.235 mm diameter) was used to print the conductive materials. No layer

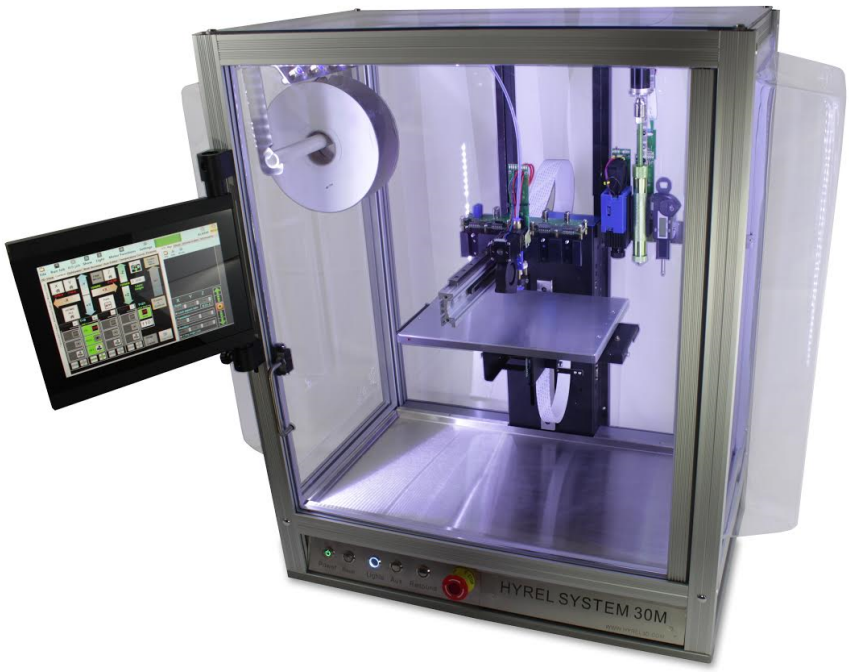

Figure 1: Hyrel System 30M

correction was needed as the conductive material was only printed in a single layer as the very top of the printed plastic. The top print layer was ensured to be level due to the above theory on print bed unevenness absorption.

The ST-1 is a 5000 rpm spindle tool that can accept any ER-11A collet and thus a wide variety of tools. While traditionally used for milling and drilling, in this case the ST-1 was used to hold a vinyl cutting drag knife that will be shown later.

Table 1: Tool summary for research use

Tool	Materials	Resolution
MK1-250	Thermoplastic Polymers	Nozzle ϕ 0.5mm
SDS-5	Assorted Liquids/Pastes	Standard Leur Lock Needle Gauges
ST-1	N/A	Standard Drill/Mill Sizes

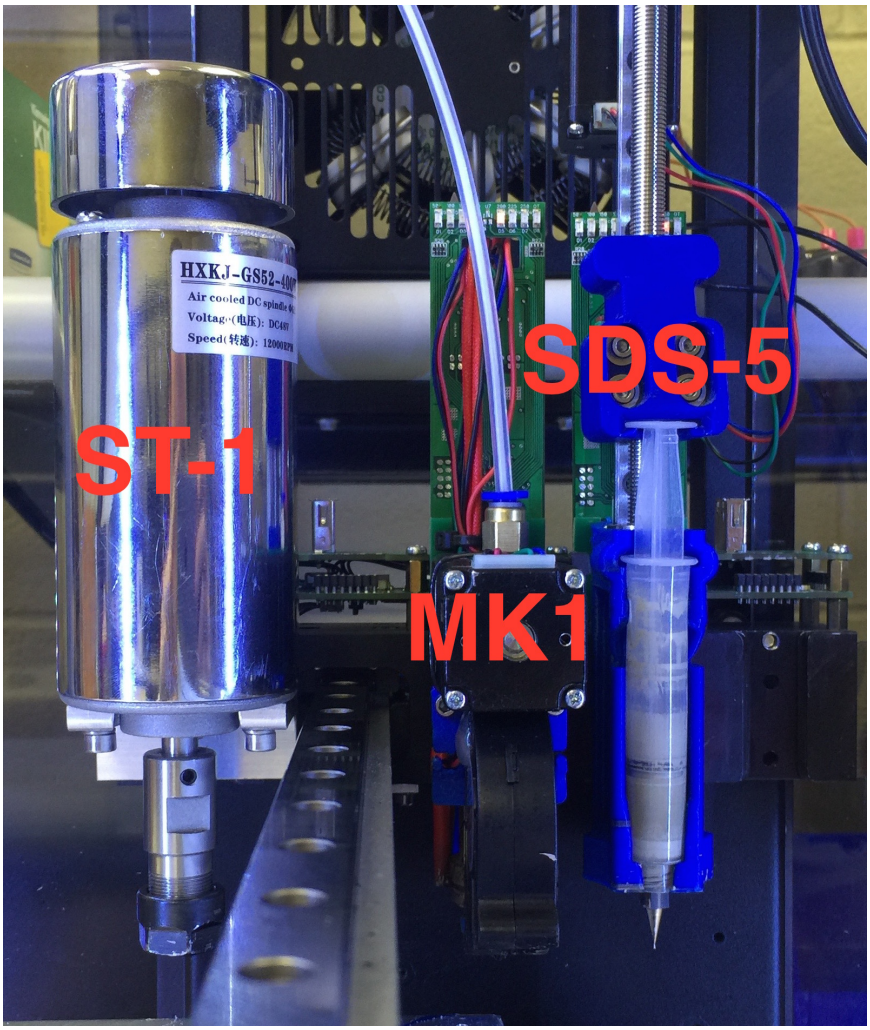

Figure 2: Toolheads used for research effort

3.1.2 Conductors

There are a wide variety of conductive materials that can be printed including conductively loaded polymers and metallic inks. This research was focused on RF structures so high conductivity materials were desired. Building on previous research efforts [8, 15] the two printed conductive materials selected for deposition were DuPont CB028 and Electroninks Diamine Silver Acetate. As highlighted earlier, material extrusion is time consuming and inefficient for large areas. For this reason, copper tape is used in these large surface area conductors in order to reduce fabrication time and cost.

3.1.2.1 CB028

DuPont CB028 is a silver loaded paste traditionally used for screen printing. The silver loading is 60-70%, making it a highly conductive material that can be used for the electronics structures described in this research even without a sintering (annealing) process. Previous work in [8] has highlighted the conductivity of the material over a variety of curing processes. The estimated conductivity is 5-10% of bulk silver without sintering.

3.1.2.2 Diamine Silver Acetate

Diamine silver acetate (DSA) is a silver solution that after evaporation leaves behind a pure silver trace. Due to the special curing process it has a higher conductivity than the CB028 or other loaded pastes or inks; however, the silver is low viscosity and low silver wt% making the printed conductors incredibly thin. The sheet resistance for DSA is substantial despite the high conductivity and it does not print controllably, often bleeding across the surface of the printed polymers in an uncontrolled manner. For these reasons, it was determined that DSA was not appropriate to move forward in this research.

3.1.2.3 Copper Tape

Copper tape is often used as a very rough prototyping material or a "band-aid" for electronic circuit fabrication, in particular in the research domain. It is readily available, relatively cheap, very thin (0.002") and highly conductive ($\sigma = 5.9E7\ S/m$). All of these factors play into making it a superior large area conductor in comparison to printing large area conductors out of silver material. Copper tape is superior for use in ground planes and large conductor structures that would otherwise be costly in terms of time for printing and material volume used.

3.1.3 Dielectrics

Acrylonitrile Butadiene Styrene (ABS) is a low-cost and commonly available thermoplastic polymer used in a wide variety of industrial and commercial applications. It is also one of the most commonly used polymers for material extrusion. There are a wide variety of providers of ABS printing filament making it a commodity and in turn driving down prices. Nominal electronic material property ranges for ABS are taken from [10] and listed below in Table 2. This work is also cross-referenced with later work in [8] in which ABS was more stringently tested over variables such as color. Non-colored ABS was used for this research and as such the expected material properties used for simulation are provided

Table 2: ABS Material Properties

Measured ABS Properties [10]		Modeled Properties
Relative Permittivity	2.54-2.79	2.5
Loss Tangent	0.0067-0.0106	0.008

The material variations seen in literature are due to a variety of factors:

- There are many different companies producing ABS, each using a slightly different method and slightly different filler materials
- ABS is first and foremost used to create mechanical structures making the electrical properties an afterthought
- Different test methods across different universities have varying uncertainty in the values

At the time of this writing, there is not a company of a Rogers or Taconic level creating plastic for AM in a controlled and well tested manner. Thus, the values provided in literature must be taken as a rough idea and not the absolute truth as they are often treated.

3.2 Hybrid Manufacturing Process

In general, the hybrid manufacturing process is broken down into two categories: additive manufacturing processes and subtractive manufacturing processes. The additive processes are composed of dielectric and conductor printing while the subtractive processes focus on selective removal of copper tape.

3.2.1 Additive Manufacturing Process

Both the MK1-250 and the SDS-5 are used to selectively deposit ABS and CB028, respectively, where required and to build up the structure as desired. Fully-printed RF/electronics structures are realized by iterating each of these two steps until the desired structure is complete.

It is worth stating that there are many small variables that can affect the quality of a printed structure. To name a few, these may include layer height, print speed & acceleration, extrusion width, bed temperature, nozzle temperature, printed bead overlap %, and cooling fan speed. As an illustrative example, to create a completely solid layer, the nozzle must pass over the entire area of the layer shape. There are an infinite number of ways for the nozzle to fill in the entire area; however, for the purposes of this research only two methods were used for polymer deposition: rectilinear and concentric, shown in Fig. 3. Rectilinear infill makes back and forth passes in a rectilinear grid with overlapping layers occurring 90^o offset from each other. The concentric infill scales down the outermost perimeter in concentric patterns. The study of the different printing parameters is outside the scope of this research; however, it is worth noting for future research the basic printing parameters used. These can be found in Appendix A.

3.2.1.1 Polymer Deposition

ABS thermoplastic polymer is deposited by the MK1-250 Hyrel toolhead. It utilizes the standard method of deposition known as material extrusion (ME) or more

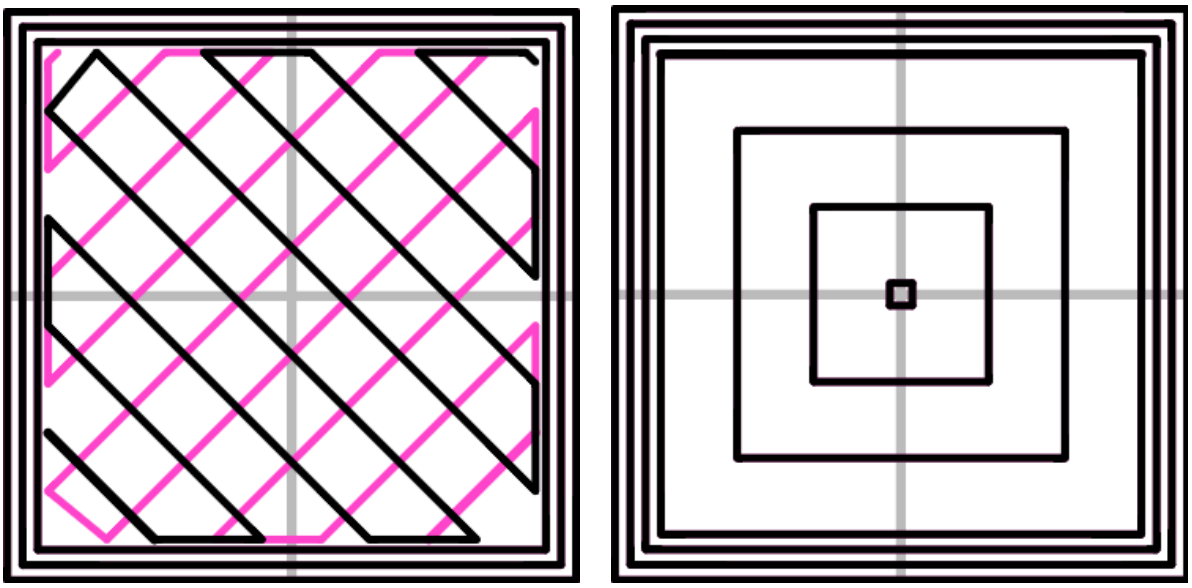

(a) Rectilinear infill (45^o) (b) Concentric infill

Figure 3: Standard Slic3r infill patterns [19]

commonly known as fused deposition modeling (FDM) or fused filament fabrication (FFF). In this process, a strand of pre-extruded 1.75 mm ABS plastic is passed through a heated chamber ($190^oCto250^oC$) and extruded through a small opening. The MK1-250 nozzle is approximately 0.5 mm.

Once extruded, the molten plastic then either sticks to the heated build plate (in the case of the first layer) or sticks to the already printed layer of plastic below (in the case of layers #2 - #N, where N is the total number of layers). 3D structures can then be built up in this manner, layer by layer, into arbitrary shapes.

One of the difficulties of FFF is humping that may occur from printed beads not completely overlapping with each other. An illustration is given in Fig. 5. This is generally accepted and not a large concern for many of the prints that are traditionally done. For RF components, these rough surfaces may translate to an increase in loss and even impedance matching issues as a trace travels over the humps. Various surface smoothing techniques were explored in [8]. It was concluded in the end that the best technique to mitigate this issue was tuning the printing parameters to produce the

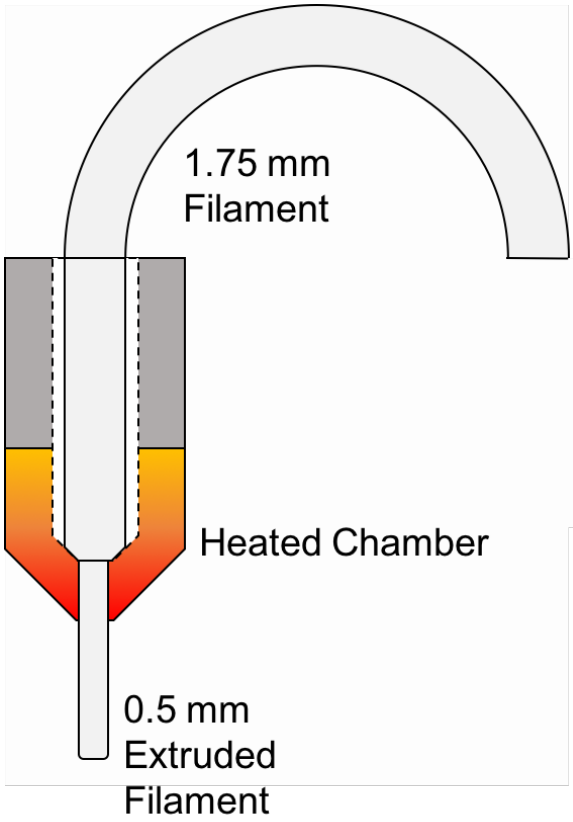

Figure 4: Illustration of material extrusion

smoothest surface possible.

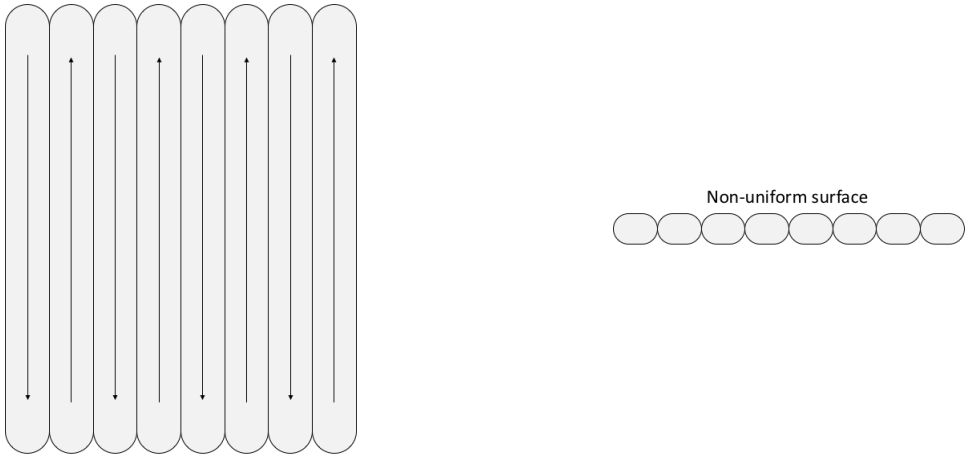

(a) Printed beads with print direction (b) Printed beads, longitudinal view

Figure 5: Printed beads showing humping behavior

An in-depth study of the surface roughness was not performed as part of this research. It was noted, however, that a concentric top layer print direction and a smaller bead width (extrusion width) helped lower the local surface roughness present in a print. These parameters are captured in the print settings in Appendix A.

3.2.1.2 Silver Depostion

The silver materials are deposited by loading a 5 mL syringe with the desired silver material (CB028 or DSA) and loading the syringe into the SDS-5. Once in the toolhead, the syringe can be driven by a stepper motor to push or pull the plunger as needed to control material flow.

A special 30 gauge stainless steel tapered needle was used (provided by Precision Valve & Automation, Inc.) for silver dispensation. This needle was selected over a standard straight needle to allow for a smoother flow of the more viscous CB028 material. The silver was dispensed in a single layer with the intended height of 0.100 mm. Special print settings were used for the silver printing. These are captured in

Appendix B.

Figure 6: PVA Tapered Needles

3.2.2 Subtractive Manufacturing Process

The subtractive process explored is the selective removal of copper tape from an area. This is achieved with a spring loaded, carbide steel, vinyl cutter blade that can be loaded into the Hyrel ST-1 with an ER-11A $\frac{1}{4}$ inch collet. A silhouette of the desired ground configuration can then be CNC cut and removed, providing incredible accuracy for a copper tape structure that could not be realized if trying to cut by hand. Additionally, this method is far faster and cheaper than printing a silver ground structure due to the fact that only a single pass of the tool is needed to cut the silhouette and the material used is copper instead of silver.

For this process, a DXF (Drawing Exchange Format) file of the intended shape to cut is generated. This DXF is then processed in Hyrel's software and turned into a toolpath to cut the desired shape out of the copper tape. Manual removal of the undesired copper tape is required at this time. Once the copper has been properly prepared printing can commence again, building on top of the structure.

Figure 7: Tormach Drag Knife

CHAPTER IV

HYBRID MANUFACTURED RADIATOR FABRICATION AND RESULTS

4.1 Patch Antenna

The inset-fed patch antenna was selected as an ideal candidate to test out the materials and processes outlined above. It is susceptible to material variations due to its high Q nature and so should act as a good meter of manufacturability and repeatability. It is also a metal-insulator-metal structure meaning it would utilize all the materials outlined and thus operate as a good test to determine how well the materials interact together. Finally, it is a well understood and used example, making it an appropriate example that can be easily processed and understood in the literature.

A simple inset-fed patch antenna was designed using HFSS antenna design kit. The antenna design kit is an Ansys built tool that synthesizes and pre-builds an initial model for specific antenna types. The inset patch was synthesized for a center frequency of 6 GHz, a substrate thickness of 0.9mm and a substrate permittivity of $\epsilon_r = 2.5$ and loss tangent 0.008. No antenna optimization was performed in order to illustrate the ease in which an antenna could be synthesized and then nearly instantly printed. The only modification was in changing the patch's conductivity to reflect the slightly lower conductivity of the printed silver. This highlights the capability of the printing process to print simple structures that can be modeled easily.

The patch antenna manufacturing process contained the following steps in this order and is illustrated in Fig. 9:

1. ABS deposition

2. Silver deposition

3. Copper tape ground plane application

First, the CAD model was exported from HFSS as 3D STL files for printing. ABS was then deposited to provide the substrate using the exported STL files. An individual layer height of 0.3 mm for a total of 3 layers yielded a nominal substrate thickness of 0.9 mm. It is important to have the total thickness be an integer multiple of the single layer printing thickness. This will ensure reliable results when printing substrates.

Once the ABS was printed silver CB028 was loaded into the SDS-5 and printed on top of the substrate using an STL file for the patch. For the purposes of this patch, a concentric infill pattern was used to ensure adequate coverage of the desired metallic areas. A single layer of CB028 was printed at a nominal thickness of 0.1 mm. This is much thicker than traditional half-ounce copper (about 0.02 mm thick) but is required in order to ensure proper coverage of the metallic area.

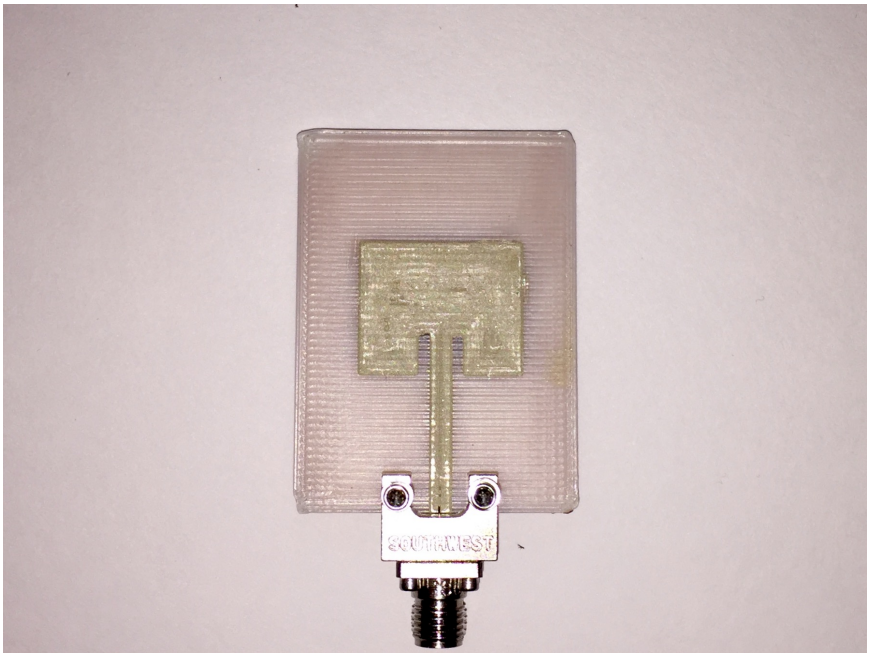

Figure 8: Successfully printed patch antenna

After the CB028 was printed, the printed antenna was removed from the bed of the printer and copper tape was manually applied to the underside. This provided a low-cost and fast ground plane for the patch antenna to operate above and required minimal processing. It would be possible to have a fully printed CB028 ground plane; however, due to the slow nature of ME and the relatively high-cost of silver it is far more useful and economical to utilize copper tape in places where large ground structures are required.

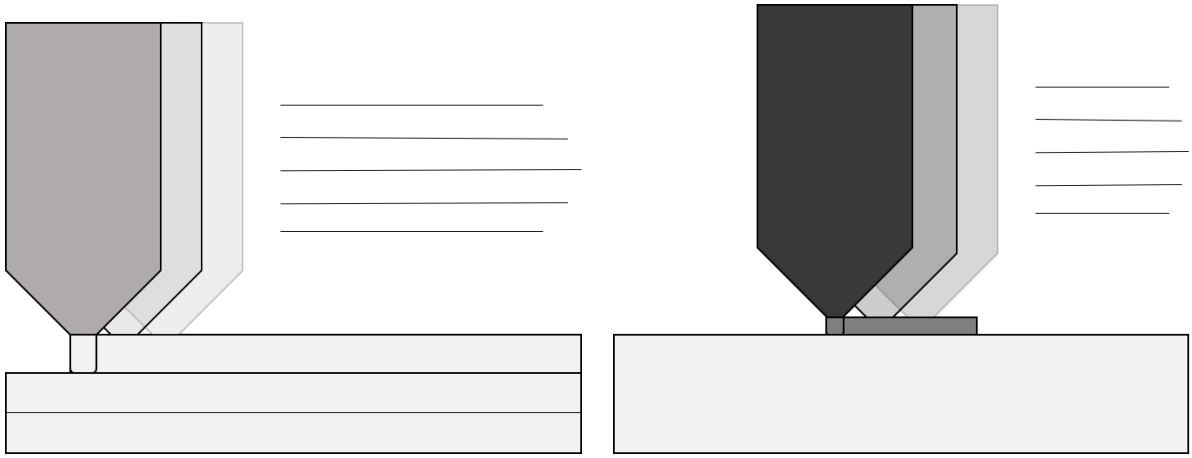

(a) RF substrate printing (b) Silver patch printing

Figure 9: Additive manufacturing printing process

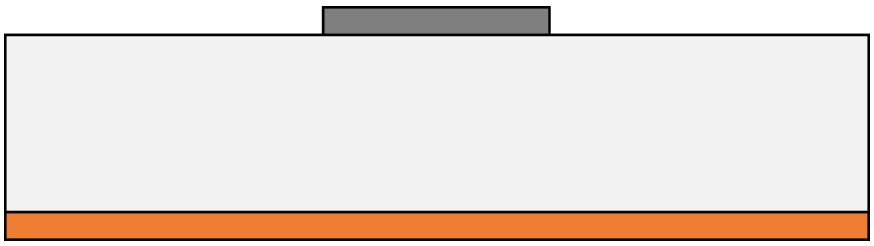

Figure 10: Final additively manufactured result

The return loss values for multiple printed patch prototypes can be seen in Fig. 11. Multiple patches were printed to show repeatability in the printing process. All three of the printed antennas operate well at the 6 GHz target frequency but are tuned slightly out of band. It is expected that this frequency issue can be attributed to the lack of a reliable RF quality thermoplastic supplier for 3D printing filament. Even a

slight variation in relative permittivity (e.g. 2.7 instead of 2.6) could cause this slight frequency shift for a patch antenna.

The antenna was tested in an az-over-el coordinate system at the Georgia Tech Research Institute shown in Fig. 13. Principal plane cuts were taken of the patch antenna in order to compare its measured patterns with modeled patterns from HFSS. Fig. 12 shows the modeled and measured patch antenna patterns. The H-plane pattern shows good agreement across the full cut with the exception of the backlobe. This discrepancy is likely due the test setup and how the antenna was oriented with the positioner. The E-plane cut also agrees well with the modeled pattern; however, this shows much more variation than the model predicted. This impact can be attributed to two primary factors: the Southwest Microwave clamp-on connector and the test setup. The coaxial connector and the roll positioner are both in the line of the E-plane cut and thus would have a much more significant effect than on the H-plane cut.

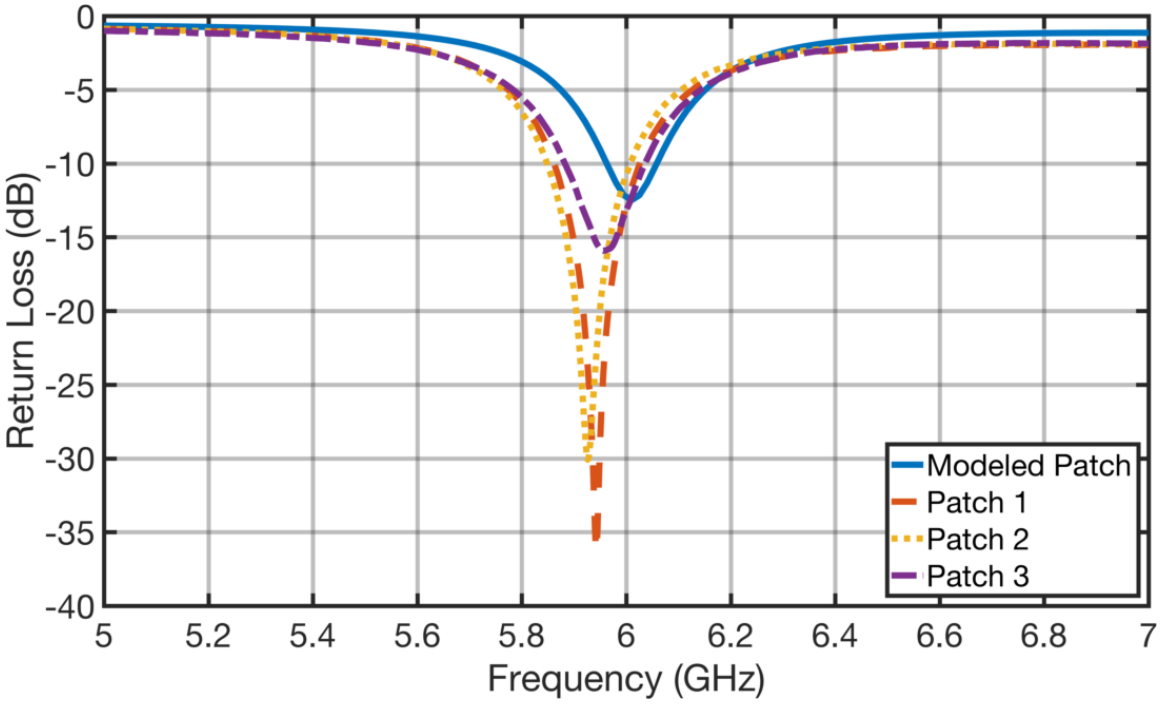

Figure 11: Return loss of multiple printed patch prototypes

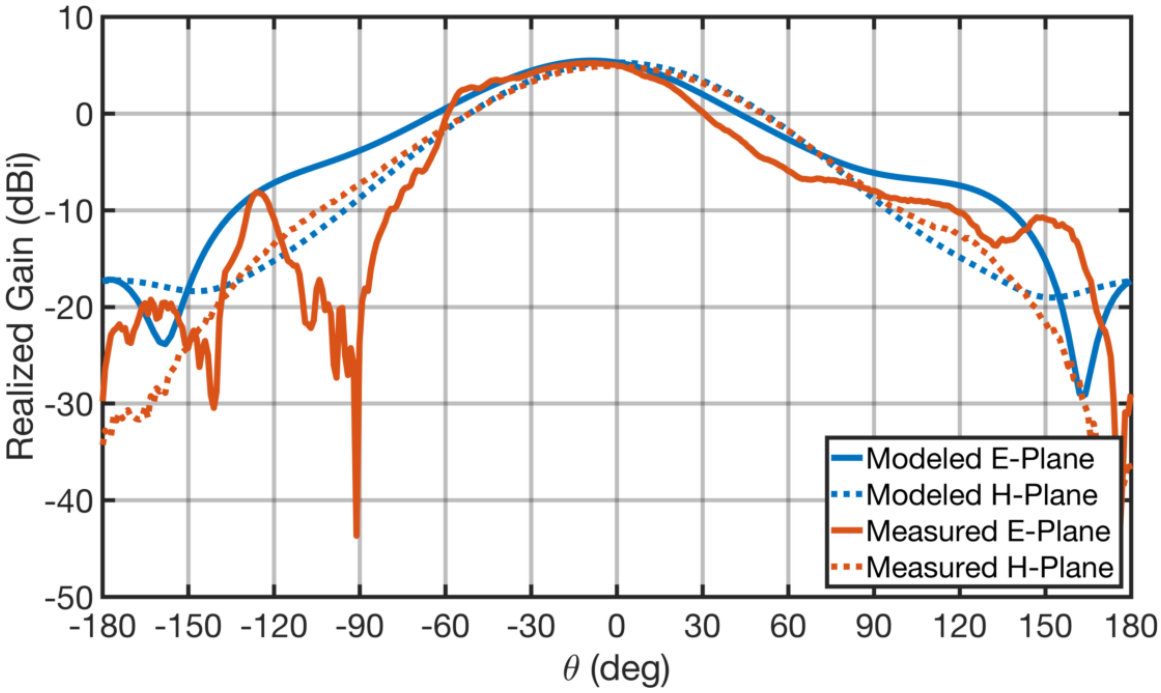

Figure 12: Printed patch antenna patterns

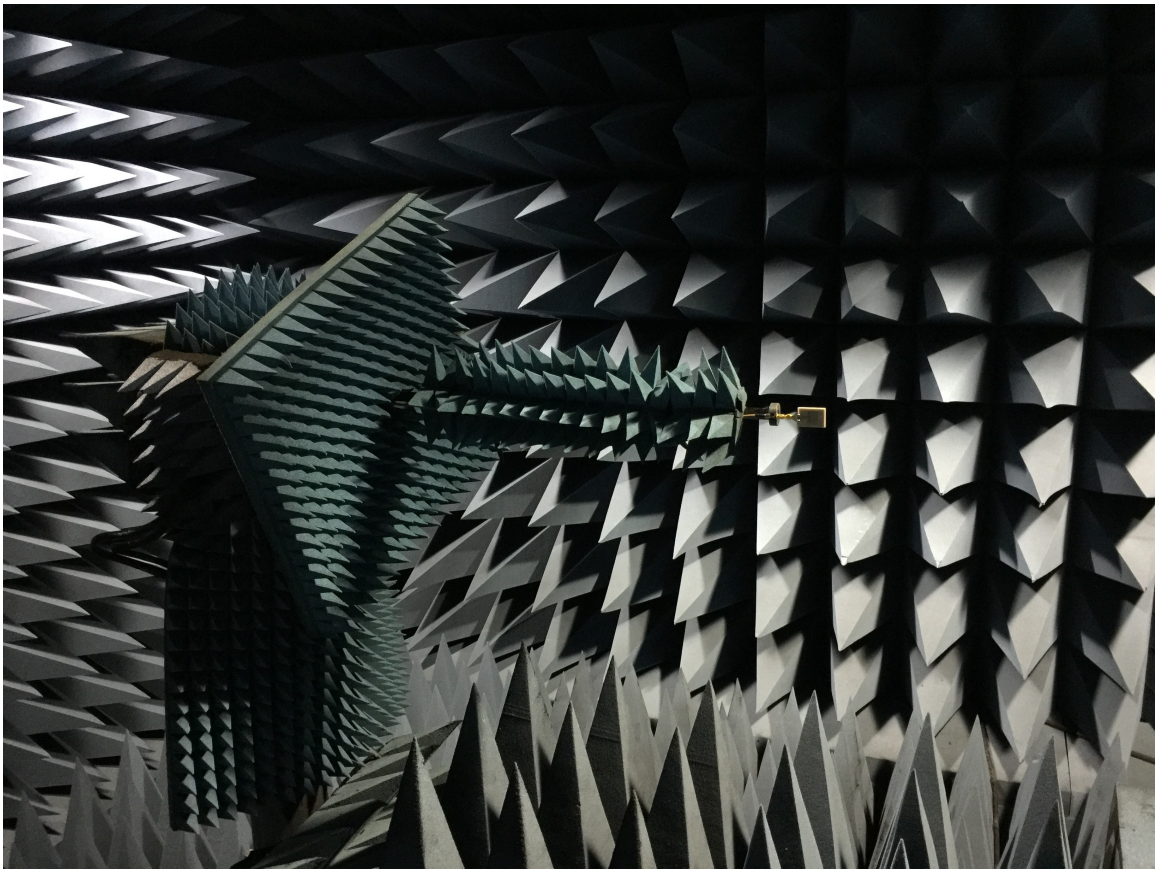

Figure 13: Patch antenna on roll-over-az positioner

4.2 Vivaldi Array

The Vivaldi element was selected as the best example to demonstrate multiple facets of the research. It simultaneously tackled:

1. Hybrid manufacturing
2. Rapid prototyping development
3. Starting with a canonical design

It is also a metal-insulator-metal structure that would iterate and demonstrate a new capability beyond the patch antenna previously.

The Vivaldi antenna array manufacturing process contained the following steps in this order and further illustrated in Fig. 14:

1. ABS deposition
2. Copper tape application
3. Copper taper cutting
4. Copper tape removal
5. ABS deposition
6. Silver deposition

First, the Vivaldi antenna element was simulated in HFSS in an infinite array environment. This allowed for quick simulation time to reduce the development time. Once a suitable model was generated it was exported as a .SAT file (2007 version) and brought into SolidWorks. Once in SolidWorks, separate .STL files were generated for the base substrate, RF substrate and silver traces. A DXF was generated for the Vivaldi shape to generate the tool path of the drag knife.

Once all the files were appropriately generated, the manufacturing process steps outlined in Fig. 14 were performed. First, the base substrate was printed from the generated STL file. This provided a plastic layer for the adhesive side of the copper tape to stick to.

After the base layer was printed, a strip of copper tape was manually laid down on top of the base layer. Firm pressure was applied to ensure adequate adhesion between the copper tape and the base substrate. Next the drag knife was used to cut the copper tape into the Vivaldi taper shape. After the tape was cut, the negative pieces were manually removed leaving behind just the copper tape in the desired tapered shape.

Before printing the RF substrate, the copper tape was cleaned with high proof isopropyl alcohol. Plastic adhesive (Aquanet brand hairspray) was applied to help the subsequent layer of ABS adhere to the top of the copper tape. The RF layer of ABS material was then printed and the top layer was smoothed and cleaned with a razor blade, removing any minor imperfections.

Finally, the silver syringe was loaded into the SDS-5 and allowed to come to room temperature (about 5 minutes). Once at the standard temperature, the silver was printed by slicing the trace STL file for a single printing layer. The needle used was a Precision Valve and Automation 30 gauge tapered stainless steel needle with the extra tip removed. The extra tip is extremely fragile and ultimately was found to not improve the performance of the silver printing. It is critical to use a tapered needle, however, as this helps in the printing of the thick and viscous CB028.

A finished Vivaldi array prototype is shown in Fig. 17 and 18. Southwest clamp on style connectors were used to connect coaxial cables to the traces for return loss and radiation pattern testing and validation. The return loss data can be seen in Fig. 16. The array was designed for a bandwidth of 4 GHz centered at 5.0 GHz which is reflected in the infinite array return loss. However, due to finite array effects

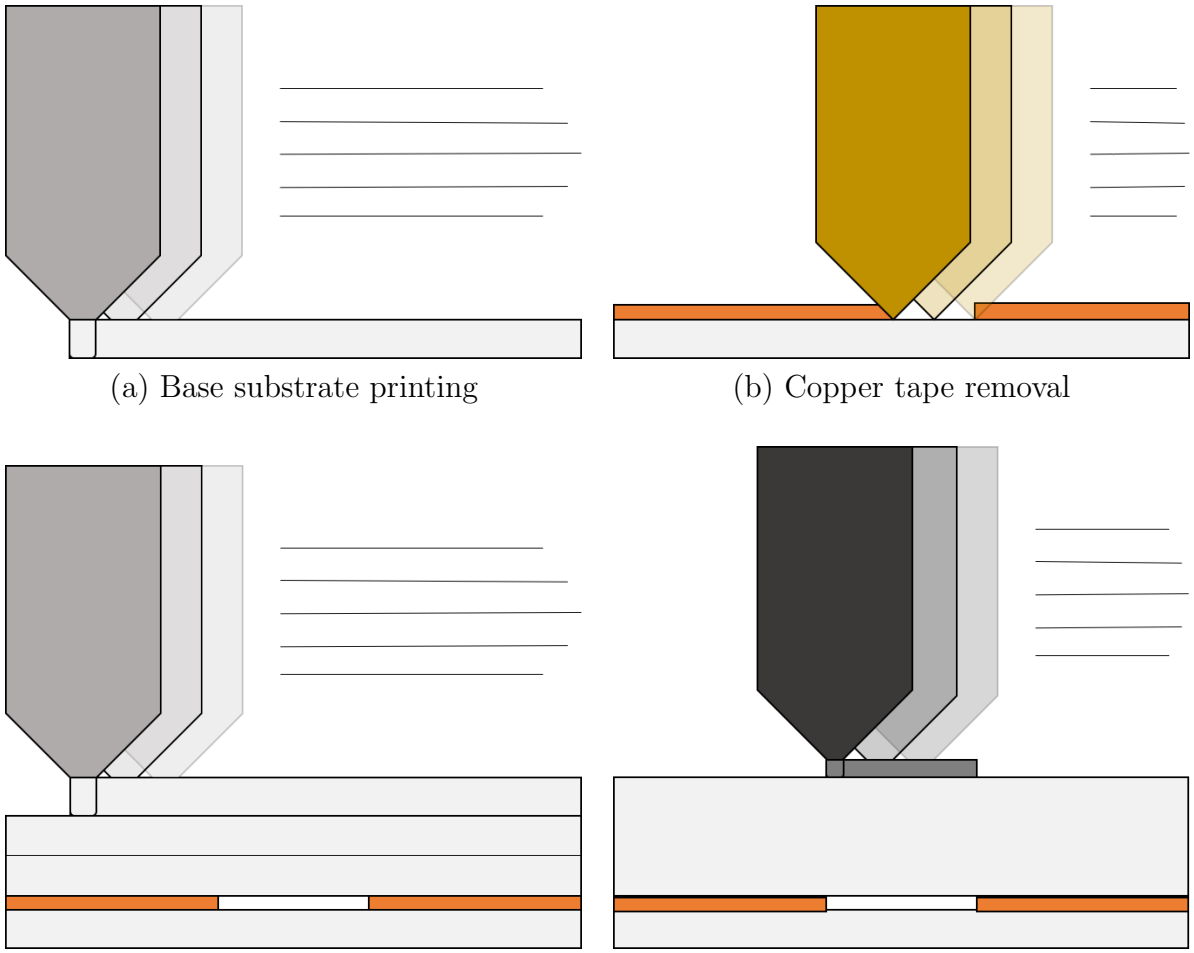

(a) Base substrate printing

(b) Copper tape removal

(c) RF substrate printing

(d) Silver trace printing

Figure 14: Hybrid manufacturing steps for Vivaldi antenna

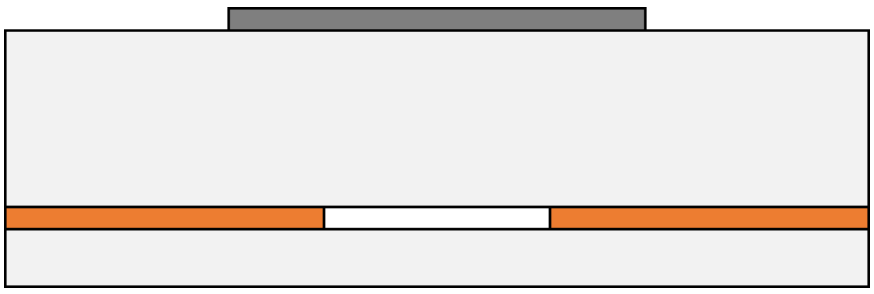

Figure 15: Final hybrid manufactured results

the eventual return loss seen in the eight element array has a significantly reduced bandwidth. Despite this, the array performs well in the 6 GHz region as can be seen in the radiation pattern testing.

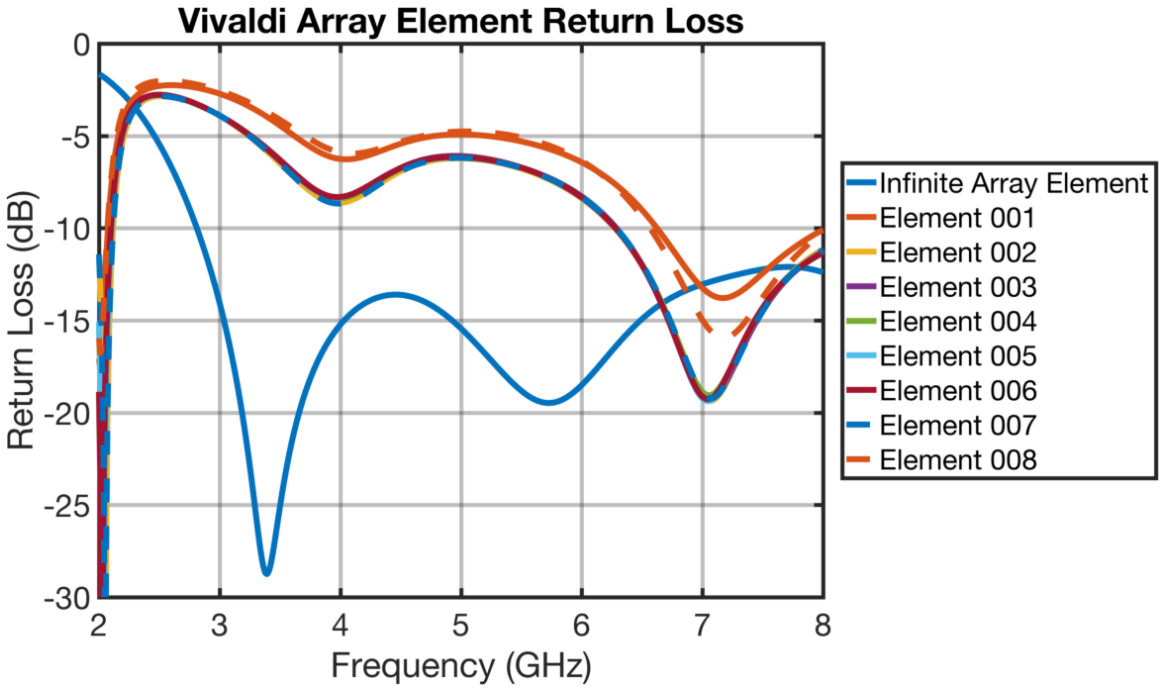

Figure 16: Vivaldi Array Return Loss

The array placement in the test environment is shown in Fig. 19 first in the orientation for an E-plane scan and then a wider angle to show the full roll-over-az antenna test positioner. The array was tested at the same anechoic chamber as the patch antenna.

Principal plane cuts were measured for each element of the array and results are shown in Fig. 21. Very good agreement is seen between the HFSS finite array model and the measured patterns with two exceptions. First, the E-plane measurements exhibit an interference pattern that is not seen in the H-plane. This is likely due to the way in which the array was mounted to the positioner which, as seen in Fig. 19, is in the same plane as the E-plane of the array. Second, for element 008 a very poor response in the measured H-plane is seen. This is most likely due to some testing

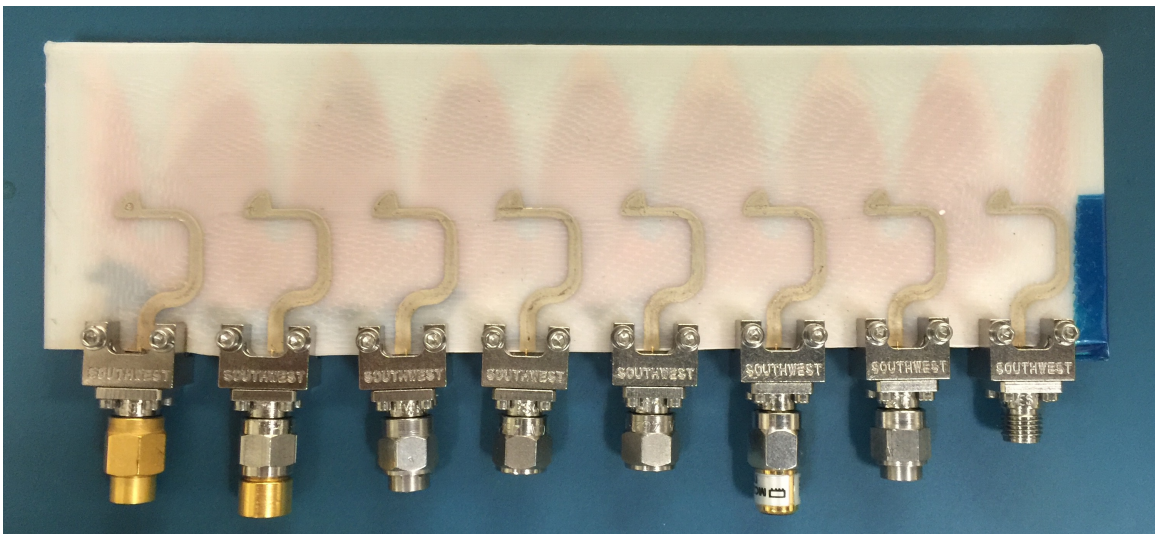

Figure 17: Hybrid Manufactured Vivaldi Array - Top

Figure 18: Hybrid Manufactured Vivaldi Array - Bottom

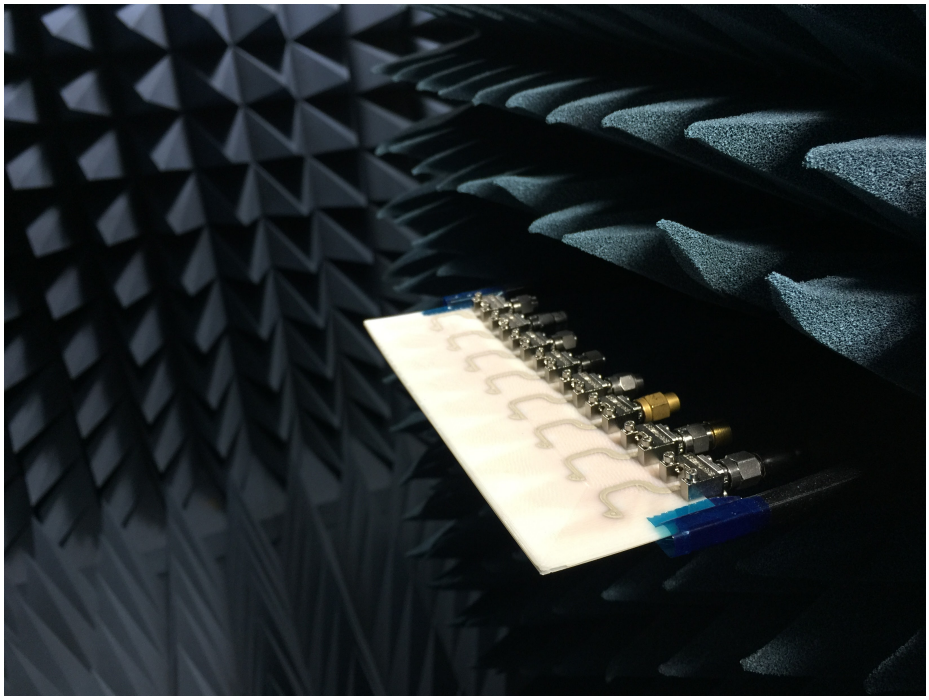

Figure 19: Array in E-plane test orientation

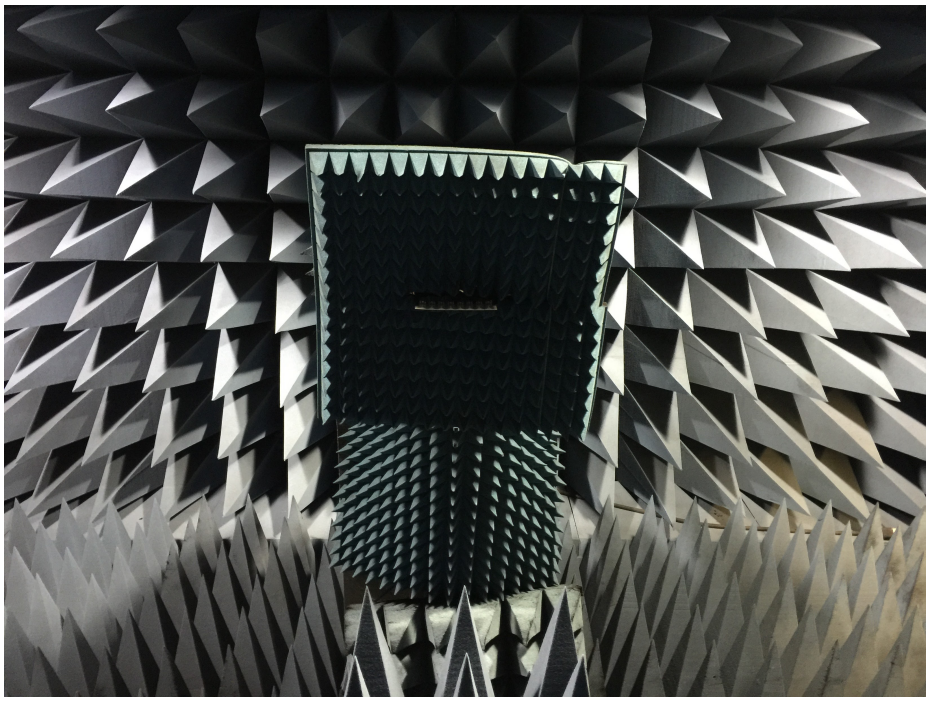

Figure 20: Array with full roll-over-az positioner

error where the connector was not properly attached. The E-plane measurements line up with with the modeled patterns showing that for at least one of the scans the element operated correctly. Unfortunately, due to time and cost constraints, more testing could not be completed to verify the element 8 H-plane pattern.

4.3 Conclusions

The data show good agreement between the model and fabricated samples for both the inset fed patch antenna and the wideband Vivaldi array. Verification of the fabrication process is exhibited in the closeness of the data. Small difference are exhibited and are likely due to material variations, slight printing errors (both dielectric and conductor) and finite array effects. It is believed, despite the errors, that the fabrication process has been borne out and proven to operate well for the intended applications.

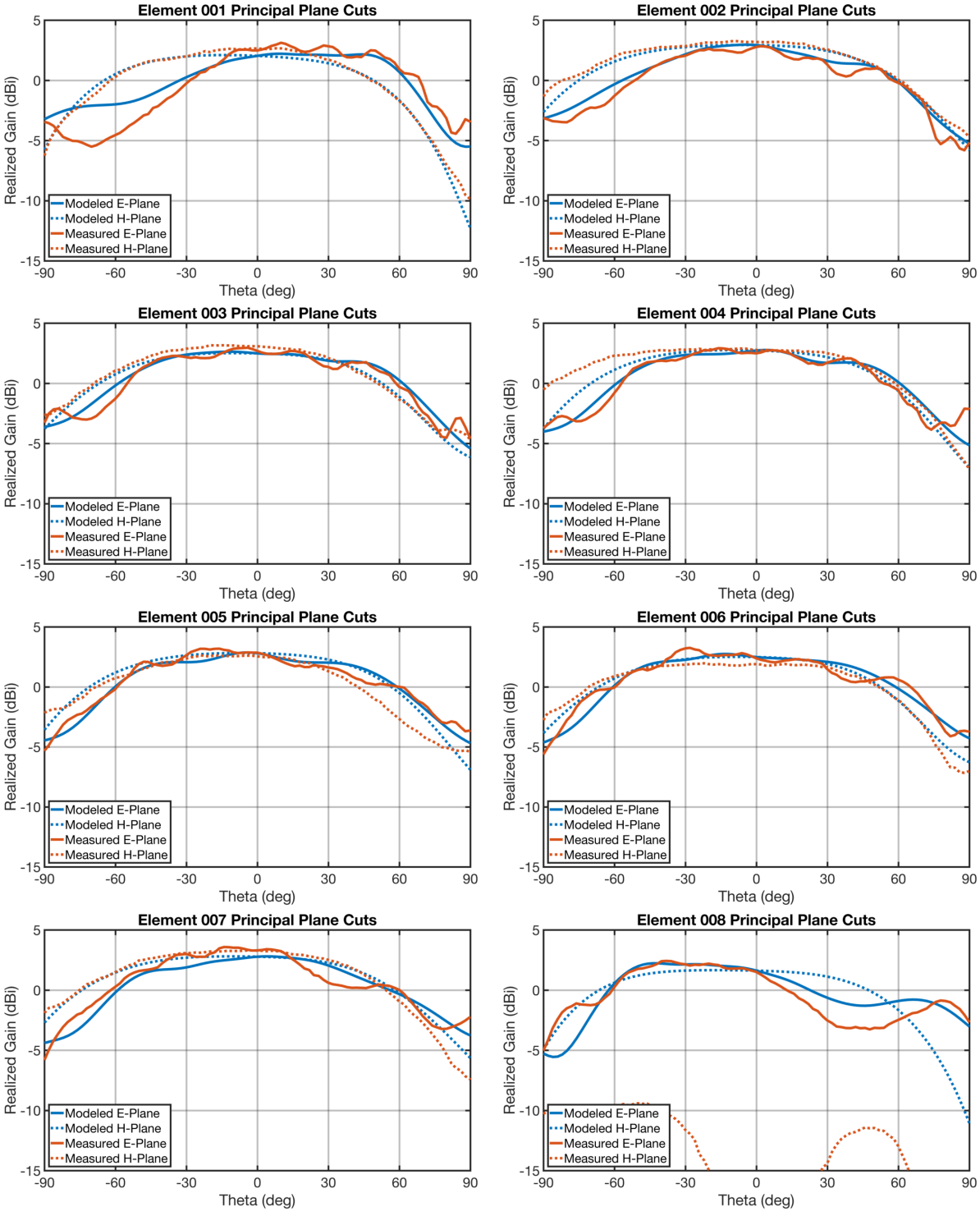

Figure 21: Array element pattern principal plane cuts

CHAPTER V

CONCLUSION

Additive manufacturing is increasingly touching all aspects of the world. These applications range from automotive to aerospace to electronics bringing the same benefits of rapid prototyping and low-cost, low-volume production to each domain. Despite this, a more novel approach is needed for printed electronics due to the typical high-cost of the precision and materials required. Hybrid manufacturing, through an intelligent combination of additive and subtractive techniques, is an ideal method to realize many of these electronic needs.

A 6 GHz patch antenna was designed, fabricated and tested as a proof of concept for low-cost, single-platform manufacturing of an RF component. Multiple antennas were fabricated, each operating within spec and matching the return loss and principal plane radiation pattern cuts of the modeled antenna. The HFSS antenna design kit was also used to design the antenna. This showed a basic workflow that could be used to rapidly generate antenna designs and realize them in less than an hour.

After the success demonstrated by the patch antenna, a more rigorous and difficult design was attempted in a wideband Vivaldi antenna array. A single Vivaldi antenna element was designed and optimized in HFSS in an infinite array environment and then simulated as an eight element finite array without additional optimization. The Vivaldi antenna highlighted the strong benefits of using additive and subtractive manufacturing on a single-platform. By using a combination of printing and cutting a full array with high conductivity metals was realized.

Hybrid manufacturing combines the custom nature of additive manufacturing with the high resolution and tolerances that we've come to expect from all traditional

manufacturing. Additionally, a single-platform machine can produce custom parts with the required resolution and repeatability needed for RF electronics. While it is unlikely that fully printed electronics will be able to compete on cost with traditional PCBs, hybrid manufacturing will help reduce that gap and in turn bring printing even closer to realizing completely novel fully 3D system-integrated RF electronic designs.

APPENDIX A

ABS PRINT SETTINGS

These are the Slic3r configuration file settings used for printing all the dielectrics used in this research.

```
avoid_crossing_perimeters = 0
bottom_solid_layers = 0
bridge_acceleration = 1000
bridge_flow_ratio = 1
bridge_speed = 20
brim_width = 0
complete_objects = 0
default_acceleration = 1000
dont_support_bridges = 0
external_fill_pattern = rectilinear
external_perimeter_extrusion_width = 0.55
external_perimeter_speed = 30
external_perimeters_first = 1
extra_perimeters = 1
extruder_clearance_height = 20
extruder_clearance_radius = 20
extrusion_width = 0.55
fill_angle = 0
fill_density = 100%
fill_pattern = rectilinear
```

```
first_layer_acceleration = 1000
first_layer_extrusion_width = 0.55
first_layer_height = 0.3
first_layer_speed = 30
gap_fill_speed = 15
gcode_comments = 1
infill_acceleration = 1000
infill_every_layers = 1
infill_extruder = 1
infill_extrusion_width = 0.55
infill_first = 0
infill_only_where_needed = 0
infill_overlap = 15%
infill_speed = 30
interface_shells = 0
layer_height = 0.3
max_print_speed = 60
max_volumetric_speed = 0
min_skirt_length = 0
notes =
only_retract_when_crossing_perimeters = 1
ooze_prevention = 0
output_filename_format = [date]_[time]_[input_filename_base].gcode
overhangs = 1
perimeter_acceleration = 1000
perimeter_extruder = 1
perimeter_extrusion_width = 0.55
```

```
perimeter_speed = 30
perimeters = 2
post_process =
raft_layers = 0
resolution = 0
seam_position = aligned
skirt_distance = 10
skirt_height = 1
skirts = 5
small_perimeter_speed = 30
solid_infill_below_area = 0
solid_infill_every_layers = 0
solid_infill_extruder = 1
solid_infill_extrusion_width = 0.55
solid_infill_speed = 30
spiral_vase = 0
standby_temperature_delta = -5
support_material = 0
support_material_angle = 0
support_material_contact_distance = 0
support_material_enforce_layers = 0
support_material_extruder = 1
support_material_extrusion_width = 0
support_material_interface_extruder = 1
support_material_interface_layers = 3
support_material_interface_spacing = 0.3
support_material_interface_speed = 100%
```

```
support_material_pattern = rectilinear
support_material_spacing = 2.5
support_material_speed = 30
support_material_threshold = 0
thin_walls = 1
threads = 8
top_infill_extrusion_width = 0.55
top_solid_infill_speed = 20
top_solid_layers = 0
travel_speed = 30
xy_size_compensation = 0
```

APPENDIX B

CB028 PRINT SETTINGS

These are the Slic3r configuration file settings used for printing all the CB028 conductors used in this research.

```
avoid_crossing_perimeters = 0
bottom_solid_layers = 0
bridge_acceleration = 0
bridge_flow_ratio = 1
bridge_speed = 5
brim_width = 0
complete_objects = 0
default_acceleration = 0
dont_support_bridges = 0
external_fill_pattern = rectilinear
external_perimeter_extrusion_width = 0.235
external_perimeter_speed = 5
external_perimeters_first = 1
extra_perimeters = 1
extruder_clearance_height = 20
extruder_clearance_radius = 20
extrusion_width = 0.235
fill_angle = 0
fill_density = 100%
fill_pattern = rectilinear
```

```
first_layer_acceleration = 0
first_layer_extrusion_width = 0.235
first_layer_height = 0.1
first_layer_speed = 5
gap_fill_speed = 5
gcode_comments = 1
infill_acceleration = 0
infill_every_layers = 1
infill_extruder = 3
infill_extrusion_width = 0.2
infill_first = 0
infill_only_where_needed = 0
infill_overlap = 10%
infill_speed = 5
interface_shells = 0
layer_height = 0.1
max_print_speed = 60
max_volumetric_speed = 0
min_skirt_length = 0
notes =
only_retract_when_crossing_perimeters = 1
ooze_prevention = 0
output_filename_format = [date]_[time]_[input_filename_base].gcode
overhangs = 1
perimeter_acceleration = 0
perimeter_extruder = 3
perimeter_extrusion_width = 0.235
```

```
perimeter_speed = 5
perimeters = 2
post_process =
raft_layers = 0
resolution = 0
seam_position = aligned
skirt_distance = 10
skirt_height = 1
skirts = 3
small_perimeter_speed = 5
solid_infill_below_area = 0
solid_infill_every_layers = 1
solid_infill_extruder = 2
solid_infill_extrusion_width = 0.235
solid_infill_speed = 15
spiral_vase = 0
standby_temperature_delta = -5
support_material = 0
support_material_angle = 0
support_material_contact_distance = 0
support_material_enforce_layers = 0
support_material_extruder = 3
support_material_extrusion_width = 0
support_material_interface_extruder = 1
support_material_interface_layers = 3
support_material_interface_spacing = 0.3
support_material_interface_speed = 100%
```

```
support_material_pattern = rectilinear
support_material_spacing = 2.5
support_material_speed = 5
support_material_threshold = 0
thin_walls = 1
threads = 8
top_infill_extrusion_width = 0.235
top_solid_infill_speed = 15
top_solid_layers = 0
travel_speed = 30
xy_size_compensation = 0
```

REFERENCES

[1] Ahmadloo, M., "Design and fabrication of geometrically complicated multi-band microwave devices using a novel integrated 3d printing technique," in *2013 IEEE 22nd Conference on Electrical Performance of Electronic Packaging and Systems*, pp. 29–32, Oct 2013.

[2] Ahmadloo, M. and Mousavi, P., "A novel integrated dielectric-and-conductive ink 3d printing technique for fabrication of microwave devices," in *Microwave Symposium Digest (IMS), 2013 IEEE MTT-S International*, pp. 1–3, IEEE, 2013.

[3] Cook, B. S., Cooper, J. R., and Tentzeris, M. M., "Multi-layer rf capacitors on flexible substrates utilizing inkjet printed dielectric polymers," *IEEE Microwave and Wireless Components Letters*, vol. 23, pp. 353–355, July 2013.

[4] Cook, B. S., Mariotti, C., Cooper, J. R., Revier, D., Tehrani, B. K., Aluigi, L., Roselli, L., and Tentzeris, M. M., "Inkjet-printed, vertically-integrated, high-performance inductors and transformers on flexible lcp substrate," in *2014 IEEE MTT-S International Microwave Symposium (IMS2014)*, pp. 1–4, June 2014.

[5] Cook, B. S. and Shamim, A., "Inkjet printing of novel wideband and high gain antennas on low-cost paper substrate," *IEEE Transactions on Antennas and Propagation*, vol. 60, pp. 4148–4156, Sept 2012.

[6] Cook, B. S. and Shamim, A., "Utilizing wideband amc structures for high-gain inkjet-printed antennas on lossy paper substrate," *IEEE Antennas and Wireless Propagation Letters*, vol. 12, pp. 76–79, 2013.

[7] Coronel Jr, J. L., *Multi3D system: Advanced manufacturing through the implementation of material handling robotics*. PhD thesis, THE UNIVERSITY OF TEXAS AT EL PASO, 2015.

[8] Deffenbaugh, P., *3D printed electromagnetic transmission and electronic structures fabricated on a single platform using advanced process integration techniques*. PhD thesis.

[9] Deffenbaugh, P., Church, K., Goldfarb, J., and Chen, X., "Fully 3d printed 2.4 ghz bluetooth/wi-fi antenna," in *International Symposium on Microelectronics*, vol. 2013, pp. 000914–000920, International Microelectronics Assembly and Packaging Society, 2013.

[10] Deffenbaugh, P. I., Rumpf, R. C., and Church, K. H., "Broadband microwave frequency characterization of 3-d printed materials," *IEEE Transactions on Components, Packaging and Manufacturing Technology*, vol. 3, no. 12, pp. 2147–2155, 2013.

[11] Deffenbaugh, P. I., Weller, T. M., and Church, K. H., "Fabrication and microwave characterization of 3-d printed transmission lines," *IEEE Microwave and Wireless Components Letters*, vol. 25, no. 12, pp. 823–825, 2015.

[12] Gibson, I., Rosen, D. W., Stucker, B., and others, *Additive manufacturing technologies*, vol. 238. Springer, 2010.

[13] NanoDimension, "Nano dimension — pcb 3d printer and nanoparticle inks." `http://www.nano-di.com/`. (Accessed on 07/18/2016).

[14] NAPIM, "currentmembers." `http://www.napim.org/current-members`. (Accessed on 07/18/2016).

[15] Nate, K. A., Hester, J., Isakov, M., Bahr, R., and Tentzeris, M. M., "A fully printed multilayer aperture-coupled patch antenna using hybrid 3d / inkjet additive manufacturing technique," in *Microwave Conference (EuMC), 2015 European*, pp. 610–613, Sept 2015.

[16] Nesbitt, P. B., Tsang, H., Ketterl, T. P., Church, K., and Weller, T. M., "4 ghz 3d-printed balun-fed bowtie antenna with finite ground plane for gain and impedance matching enhancement," in *2016 IEEE 17th Annual Wireless and Microwave Technology Conference (WAMICON)*, pp. 1–3, IEEE, 2016.

[17] nScrypt, "nscrypt — 3d conformal dispensing systems & laser micro printing." `http://nscrypt.com/`. (Accessed on 07/18/2016).

[18] Olivas, R., Salas, R., Muse, D., MacDonald, E., Wicker, R., Newton, M., and Church, K., "Structural electronics through additive manufacturing and micro-dispensing," in *International Symposium on Microelectronics*, vol. 2010, pp. 000940–000946, International Microelectronics Assembly and Packaging Society, 2010.

[19] Slic3r, "Slic3r - g-code generator for 3d printers." `http://slic3r.org/`. (Accessed on 07/18/2016).

[20] Tehrani, B. K., Cook, B. S., and Tentzeris, M. M., "Inkjet printing of multilayer millimeter-wave yagi-uda antennas on flexible substrates," *IEEE Antennas and Wireless Propagation Letters*, vol. 15, pp. 143–146, 2016.

[21] Voxel8, "Voxel8." `http://www.voxel8.co/`. (Accessed on 07/18/2016).